◆ Human Brain Mapping 30:3445–3460 (2009) ◆

Time-Varied Characteristics of Acupuncture Effects in fMRI Studies

Lijun Bai,[1] Wei Qin,[1] Jie Tian,[1,2]* Peng Liu,[3] LinLing Li,[1] Peng Chen,[4] Jianping Dai,[5] Jason G. Craggs,[6] Karen M. von Deneen,[7,8] and Yijun Liu[7,8]*

[1]*Life Science Research Center, School of Electronic Engineering, Xidian University, Xi'an, Shaanxi, China*
[2]*Medical Image Processing Group, Institute of Automation, Chinese Academy of Sciences, Beijing, China*
[3]*School of Sino-Dutch Biomedical and Information Engineering, Northeastern University, Shenyang, Liaoning, China*
[4]*Beijing Traditional Chinese Medicine Hospital, Capital Medical University, Beijing, China*
[5]*Department of Radiology, Beijing Tiantan Hospital, Capital University of Medical Sciences, Beijing, China*
[6]*Clinical and Health Psychology, University of Florida, Gainesville, Florida*
[7]*Department of Psychiatry, McKnight Brain Institute, University of Florida, Gainesville, Florida*
[8]*Department of Neuroscience, McKnight Brain Institute, University of Florida, Gainesville, Florida*

Abstract: When studying the neural responses to acupuncture with a block-designed paradigm, its temporal dynamics predicted by the general linear model (GLM) conforms to typical "on-off" variations during a limited period of the experiment manipulation. Despite a lack of direct evidence associating its psychophysiological response, numerous clinical reports suggest that acupuncture can provide pain relief beyond a needling session. Therefore, a typical GLM analysis may be insensitive or inappropriate for identifying altered neural responses resulting from acupuncture. We developed a new approach to investigate the dynamics underlying sustained effects of acupuncture. Specifically, we designed two separate models to evaluate the baseline activities (prior to stimulation) and neural activities in sequential epochs, using three block-designed functional runs: acupuncture at acupoint ST36, nonmeridian point (NMP) stimulation, and a visual task. We found that the activity patterns

Contract grant sponsor: Project for the National Key Basic Research and Development Program (973); Contract grant number: 2006CB705700; Contract grant sponsor: Changjiang Scholars and Innovative Research Team in University (PCSIRT); Contract grant number: IRT0645; Contract grant sponsor: CAS Scientific Research Equipment Develop Program; Contract grant number: YZ0642, YZ200766; Contract grant sponsor: 863 Program; Contract grant number: 2008AA01Z411; Contract grant sponsor: Joint Research Fund for Overseas Chinese Young Scholars; Contract grant number: 30528027; Contract grant sponsor: National Natural Science Foundation of China; Contract grant numbers: 30873462, 90209008, 30870685, 30672690, 30600151, 60532050, 60621001; Contract grant sponsor: Beijing Natural Science Fund; Contract grant number: 4071003; Contract grant sponsor: NIH, USA; Contract grant number: NS45518; Contract grant sponsors: Chair Professors of Cheung Kong Scholars Program; Contract grant sponsor: CAS Hundred Talents Program.

Lijun Bai and Wei Qin contributed equally to this work.
*Correspondence to: Jie Tian, Life Science Research Center, School of Electronic Engineering, Xidian University, Xi'an 710071, China; Institute of Automation, Chinese Academy of Sciences, Beijing 100190, China. E-mail: tian@ieee.org; or Yijun Liu, Departments of Psychiatry and Neuroscience, McKnight Brain Institute, University of Florida, Gainesville, FL 32610. E-mail: yijunliu@ufl.edu

Received for publication 29 November 2008; Revised 9 January 2009; Accepted 7 February 2009
DOI: 10.1002/hbm.20769
Published online 6 April 2009 in Wiley InterScience (www.interscience.wiley.com).

during rest were associated with the stimulus types and that the resting activities might be even higher than that of stimulation phases. Such effects of the elevated activity during rest may reduce or eliminate the activity during stimulus conditions or even reverse the sign of brain activation using conventional GLM analysis. Moreover, such sustained responses, followed by acupuncture at ST36 and NMP, exhibited distinct patterns in wide brain structures, particularly in the limbic system and brainstem. These findings may pose great implications for the design and interpretation of a range of acupuncture neuroimaging studies. *Hum Brain Mapp 30:3445–3460, 2009.*

Key words: acupuncture; resting baseline condition; time-varied responses; functional magnetic resonance imaging

INTRODUCTION

Advances in functional neuroimaging techniques during the past few decades have opened a "window" to the human brain allowing us to study the anatomical and physiological responses associated with acupuncture [Fang et al., 2004; Hui et al., 2000, 2005; Napadow et al., 2005; Pariente et al., 2005; Wu et al., 2002]. Previous studies of acupuncture using fMRI have typically identified an attenuation or modulation of the blood oxygenation level dependent (BOLD) signal in the limbic/paralimbic, brainstem, and neocortical regions [Hui et al., 2005; Yoo et al., 2004]. This attenuation refers to a relative decrease in regional neuronal activity while an external stimulus is processed or a task is completed, compared to a baseline, or a period of "rest." Therefore, the choice of an appropriate baseline, to which the condition-related activity can be compared, is fundamental to any brain imaging study and may profoundly influence the results [Raichle et al., 2001].

According to the theory of Traditional Chinese Medicine and abundant clinical reports, the analgesic effects of acupuncture can last for an extended period of time, even several hours after the needling session [Beijing, 1980]. Psychophysical analysis from Price et al. [1984] suggests that the analgesic effects of acupuncture might actually peak long after the needling session [Price et al., 1984]. Our group is one of pioneers to focus on exploring the specific pain-related brain networks underpinning the prolonged analgesic effects of acupuncture [Bai et al., 2007; Qin et al., 2006, 2008]. According to these observations, we infer that acupuncture may induce persistent changes in neuronal activities which would extend across the interstimulus intervals (e.g., a block-based paradigm in an fMRI study). In other words, the natural increase of neural activities in response to an acupuncture stimulus may remain elevated for a prolonged period of time and not return to the prestimulation baseline level during subsequent interstimulus epochs of rest, which would confound the estimate of how much neural activity increases/decreases during subsequent epochs of stimulation. Thus, neural responses to acupuncture may not return to the baseline level during a typical fMRI experiment, which violates the assumptions upon which the typical general linear model (GLM) contrast analysis is based.

A voxel-wise application of the GLM is a standard way to analyze the BOLD signal changes in response to a stimulus (i.e., acupuncture). With this approach, a specific stimulus sequence (i.e., design matrix) is used to define an ideal hemodynamic response function (HRF), which is convolved with the actual hemodynamic response and produces predictors of the BOLD response [Worsley and Friston, 1995]. In other words, changes in the BOLD signal, evoked by a particular psychphysiological event, are completely dependent on and specific to the experimental paradigm. For a block-designed fMRI paradigm, the temporal changes in the BOLD signal as predicted by the GLM conform to the "on-off" specifications set by the experimenter.

A repetitive "on-off" stimulation pattern is generally used in fMRI studies of acupuncture because the BOLD signal change is quite small (i.e., 1–3%) and highly variable. However, as argued earlier, the inferences derived from GLM estimates are limited by the design of the experimental paradigm and whether the stimuli are under relatively precise experimental control (i.e., they can be turned on and off repeatedly). Because the effects of acupuncture may be of relatively long duration according to the Traditional Chinese Medicine, the temporal aspects of the BOLD response to acupuncture may violate the assumptions of the block-designed GLM estimates. Consequently, previous imaging studies of acupuncture may be susceptible to errors of statistical significance.

Because there is no overt task or stimulation preformed during resting-state epochs, researchers often use such epochs as the baseline against which the task activity is compared. According to the subtraction principle, a brain regions is considered "active" if the signal representing neuronal activity is greater in one condition relative to another [Gusnard et al., 2001; Kida et al., 1999]. Unlike many of the "typical" stimuli used in fMRI paradigms, acupuncture-related changes in the BOLD signal may be inherently complex and slow to develop and resolve. Therefore, the magnitude of BOLD signal in rest period following the initial stimulation is unlikely to have returned to the initial (prestimulus) baseline level, which

is a basic assumption of the subtraction technique, and is required for the results to be meaningful and accurate. Several recent fMRI studies have also recognized that, in some specific task conditions, the relaxed fixation period cannot represent a reasonable estimate of "baseline activity" due to the uncontrollable sensory or cognitive activations underlying the internal "task-like" processing [Arfanakis et al., 2000]. An alternative view is that the constant task-related stimulation may alter the underlying spontaneous BOLD fluctuations in the subsequent resting-state epochs [Arieli et al., 1996; Fox et al., 2005; Fransson, 2006].

Whatever the exact cause may be, inadequate research on acupuncture has characterized the sources of the BOLD response variability during the interleaved resting epochs and examined how these observed variations affect the statistical results of block-based fMRI studies. This study first tested the hypothesis that acupuncture, as a slow-acting agent, may account for a significant fraction of the variability in measured BOLD responses during poststimulus rest periods. To assist the interpretation of temporal characteristics of the BOLD signal changes during/after acupuncture, we examined how acupuncture stimulation-induced BOLD response was different from a standard visual task-induced response in the typical block-designed paradigm. Second, we explored the differences between the time-varied brain activities induced by acupuncture stimulation at an acupoint (ST36) and those at a nonmeridian point (NMP).

Consequently, a better understanding of how acupuncture influences the baseline neuronal activity is paramount, and should be considered a prerequisite for adopting optimal neural modeling and making reliable statistical inferences on acupuncture-associated fMRI data.

MATERIALS AND METHODS

Subjects

To reduce intersubject variabilities, participants were recruited from a group of 26 college students (13 male, ages of 21.4 ± 1.8). All the subjects were right-handed with normal or corrected-to-normal vision. The subjects were acupuncture naïve, and did not have a history of major medical illnesses, head trauma, neuropsychiatric disorders, had not used prescription medications within the last month, and did not have any contraindications for exposure to a high magnetic field. All subjects gave written, informed consent after the experimental procedures had been fully explained, and all research procedures were approved by the West China Hospital Subcommittee on Human Studies and conducted in accordance with the Declaration of Helsinki.

Acupuncture Experiment Procedures

The 26 subjects were divided into two groups in a semi-randomized order: of them 16 volunteers (8 males, ages of 21.9 ± 1.2) underwent acupuncture administration on both an acupoint ST36 and NMP (a manual acupuncture condition, ACUP; a sham acupuncture condition, SHAM), and 10 other volunteers (5 males, ages of 20.8 ± 2.1) participated in an experiment using a visual task.

In the acupuncture experiment, all subjects ($N = 16$) were blinded to the type and order of stimulations. During the procedure, subjects were instructed to keep their eyes closed to prevent them from actually observing the procedures. The presentation sequence of the ACUP and SHAM protocols was randomized across the fMRI runs, and the order of presentation was counterbalanced across subjects. To mitigate any potential long-lasting effects following the acupuncture administration, subjects were exposed to only one fMRI run per day.

Acupuncture was performed at acupoint ST36 on the right leg (Zusanli, located in the tibialis anterior muscle, four fingerbreadths below the lower margin of the patella and one fingerbreadth lateral from the anterior crest of the tibia). This is one of the most frequently used acupoints for pain analgesia and disorders of multiple systems, and has been studied in both animal and human acupuncture protocols [Beijing, 1980; Hui et al., 2005]. The needles used in the acupuncture protocol were sterile, disposable 38-gauge stainless steel acupuncture needle of 0.2 mm in diameter and 40 mm in length. The needle was inserted perpendicularly to a depth of 2–3 cm. Stimulation was then delivered by a balanced "tonifying and reducing" technique, and rotated manually clockwise and counterclockwise for 1 min at a rate of 60 times per minute. The procedure was performed by the same experienced and licensed acupuncturist on all subjects. The experimental paradigm used during the fMRI scan was an ON/OFF block design (shown in Fig. 1) that included 1 min of baseline scanning at the beginning (BL). The two stimulations epochs (A1 and A2) was separated by an interval of 1 min "rest" period (R1). Scanning was then continued for another 1 min "rest" epoch (R2) after the stimulation. This process resulted in two stimulation periods interleaved by three "rest" conditions of equal time for each period. The total scanning time was 5 min per run, and all the subjects were instructed to lie still and remain relaxed without engaging in any mental tasks.

For the control of acupuncture manipulation, subjects also received the sham stimulation at a nonmeridian focus near ST36 (approximately 2–3 cm distant laterally) on the right leg using the same timing protocol as in the ACUP run. The sham stimulation (S1 or S2) was delivered with the needle depth, stimulation intensity, and manipulation method identical to those used in the ACUP run.

At the end of each 5-min fMRI scanning, the subjects completed a questionnaire that used a 10-point visual analogue scale (VAS) to rate their experience (or "*deqi*") of aching, pressure, soreness, heaviness, fullness, warmth, coolness, numbness, tingling, dull or sharp pain they felt during the scan. The VAS was scaled as follows: 0, no sensation; 1–3, mild; 4–6, moderate; 7–8, strong; 9, severe; and 10, unbearable sensation. The questionnaire also had one

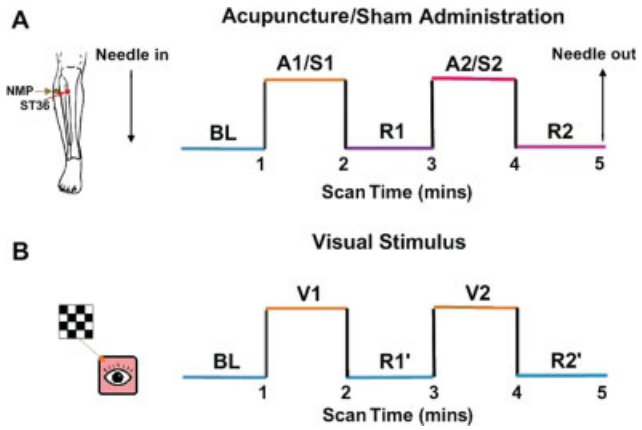

Figure 1.

Experimental paradigm. Panel **A** indicated that acupuncture needle manipulation was performed at an acupoint ST36 (Zusanli, arrow pointing to red dot) or a nonmeridian-point focus approximately 2–3 cm distant laterally (NMP, arrow pointing to green dot) on the right leg, respectively. Functional run incorporated the block design paradigm with two cycles, 1 min ON (A1/A2) and 1 min OFF (R1/R2) epoch, preceded by a 1 min baseline period (BL). For statistical analyses, the signal intensity of the BL phase served as a control baseline for detecting signal changes in the sequential four epochs. Panel **B** presented the design paradigm in the visual experiment. Visual stimulus (V1/V2) was presented for 1 min, with 1 min rest (R1′) between stimuli, preceded by a 1 min baseline BL and followed by a 1 min rest condition (R2′). Total scanning lasted for 5 min. [Color figure can be viewed in the online issue, which is available at www.interscience.wiley.com.]

blank row for subjects to add their own words if the above descriptors did not embody the sensations they experienced during the stimulation. Because sharp pain was considered an inadvertent noxious stimulation, we excluded the subjects from further analysis if they experienced sharp pain (greater than the mean by more than two standard deviations). Among the 16 participants, only one experienced the sharp pain and was removed from the further analysis.

Visual Stimulation Protocol

To assist in the interpretation of temporal characteristics of the BOLD signal changes during/after acupuncture, the visual fMRI experiment also adopted a design paradigm identical to the acupuncture described above (Fig. 1B). Visual stimuli were presented using the software "Presentation" (http://www.neurobehavioralsystems.com) that ensured synchronization with the MR scanner. A checkerboard pattern flashing of 8 Hz was used as the visual stimulus. The whole 5 min run had two cycles of 1 min visual stimulus (V1/V2) and 1 min rest scanning (R1′/R2′), preceded by a 1 min baseline period (BL). As a resting condition, a central red dot in front of the same isoluminant background was presented. The participants ($N = 10$) were instructed to focus their gaze on the center of the screen at the same position where such dot was present and to minimize blinking while the checkerboard was displayed. A computer-controlled projector system was used to display the images onto a screen placed across the bore of the magnet 3.4 m from the subjects' eyes and viewed through a prismatic mirror (10 × 15 field of view). The background luminance was held at a constant value during the length of the experiment and equaled the ambient darkness inside the bore of the MR scanner with the room light extinguished.

fMRI Scanning Procedure

Functional images were acquired on a 3T GE Signa scanner using a standard whole head coil (LX platform, gradients 40 mT/m, 150 T/m/s, GE Medical Systems, Milwaukee, WI). A custom-built head holder was used to prevent head movements. Thirty-two axial slices (FOV = 240 mm × 240 mm, matrix = 64 × 64, thickness = 5 mm), parallel to the AC-PC plane and covering the whole brain, were obtained using a T2*-weighted single-shot, gradient-recalled echo planar imaging (EPI) sequence (TR = 1,500 ms, TE = 30 ms, flip angle = 90°). The scan covered the entire brain including both the cerebellum and brainstem. Prior to the functional run, high-resolution structural information on each subject was acquired using 3D MRI sequences with a voxel size of 1 mm^3 for anatomical localization (TR = 2.7 s, TE = 3.39 ms, matrix = 256 × 256, FOV = 256 mm × 256 mm, flip angle = 7°, in-plane resolution = 1 mm × 1 mm, slice thickness = 1 mm).

fMRI Data Analysis

Initially, all the volumes of functional images were firstly realigned for head-motion corrections (none of these subjects had head movements exceeding 1 mm on any axis and head rotation greater than one degree). The image data were further processed with spatial normalization based on the MNI space and resampled at 2 mm × 2 mm × 2 mm using SPM5. Each subject's structural volumes were registered to the atlas template using a 12 parameter affine transform. The datasets were then spatially smoothed with a 6 mm full-width at half maximum (FWHM) Gaussian kernel.

Because the needle-insertion itself does not produce significant effects on acupuncture-specific fMRI signal changes [Hui et al., 2000, 2005], the resting epoch prior to acupuncture manipulation can serve as an ideal baseline (BL) for detecting changes in signal intensity during needling. To examine the reliability of the block-design protocol in modeling the predicted response of acupuncture, we specified a GLM design matrix that separates different conditions across each subject with regressors coded for the difference between the BL and subsequent four epochs, respectively. In other words, these four epochs were considered as four different conditions per session, which

generated three sequences: (1) ACUP, A1-R1-A2-R2; (2) SHAM, S1-R1-S2-R2; (3) VISUAL, V1-R1′-V2-R2′. On the basis of the abovementioned hypothesis, we assumed that if the ACUP-induced variance can sustain beyond the A1 or A2 phase, the subsequent resting epoch, i.e. the R1 or R2 phase, may retain a "continuous" acupuncture-related effect. It would be interesting to examine if the SHAM-induced variance during the S1 or S2 phase can extend to the R1 or R2 phase, so as to differentiate the temporal effect of ACUP from that of SHAM.

The statistical analyses were performed subsequently at both the individual level and group level. In the individual analysis, four *t*-contrasts were defined as follows: (1) A1 (or S1) minus BL; (2) R1 minus BL; (3) A2 (or S2) minus BL; and (4) R2 minus BL. Each of the resulting statistical maps indicated the voxel-wise signal changes for a particular condition relative to the baseline. These maps from each subject were then used to calculate one-sample *t*-test in SPM5. Statistical significance was threshold at $P < 0.005$ (uncorrected) and a minimum cluster size of three voxels. A similar procedure was also performed for the visual experiment testing with four contrasts (V1 minus BL, R1′ minus BL, V2 minus BL, R2′ minus BL). The functional imaging data were then transformed into the Talairach stereotactic space [Talairach and Tournoux, 1988], and overlaid on MRIcro (http://www.sph.s.c.edu/comd/rorden/mricro.html) for presentation purposes.

RESULTS

Psychophysical Responses

The prevalence of these sensations was expressed as the percentage of the individuals in the group that reported the given sensation (Fig. 2A). The intensity was expressed as the average score ± SE (Fig. 2B). No subject opted to add an additional descriptor in the blank row provided. The occurrence frequency of numbness, fullness, and soreness was found greater for ACUP under Fisher's exact test ($*P < 0.01$, $**P < 0.005$). Because acupuncture needle manipulations are always administrated in the tendinomuscular layers with densely distributed different nerve fibers (Aδand C), it may elicit the sensations such as soreness, numbness, and fullness. The average stimulus intensities (mean ± SE) were approximately similar during acupuncture on ST36 (2.4 ± 1.7) and NMP (2.2 ± 1.9). Average ratings of the reported six elements of *deqi* sensations (sharp pain excluded) fell between 0.6 and 4.0 on the 10.0-point scale for both ST36 and NMP. The highest scores in an individual case mainly distributed in a range of 3–7.

fMRI Results of the Visual Stimulus Versus Resting Epochs

The averaged brain activations evoked in different epochs of visual task across all subjects were summarized in Table I, and their anatomical locations were illustrated in Figure 3C. As expected, two visual epochs compared to the control fixation (contrast "V1/V2 vs. BL") produced the well-established activations specific to the occipital-temporal cortex. Significant BOLD signal increases were seen mostly in the striate cortex (BA 17), and enhanced activities in the extrastriate cortices. These regions included the middle occipital (BA 18/19), lingual (BA 18/19), and fusiform gyri (BA 18/19). Compared with the spatial activation maps of the V1, the variability of spatial distribution and signal intensity during the V2 may be partly derived from the habituation of neural responses,

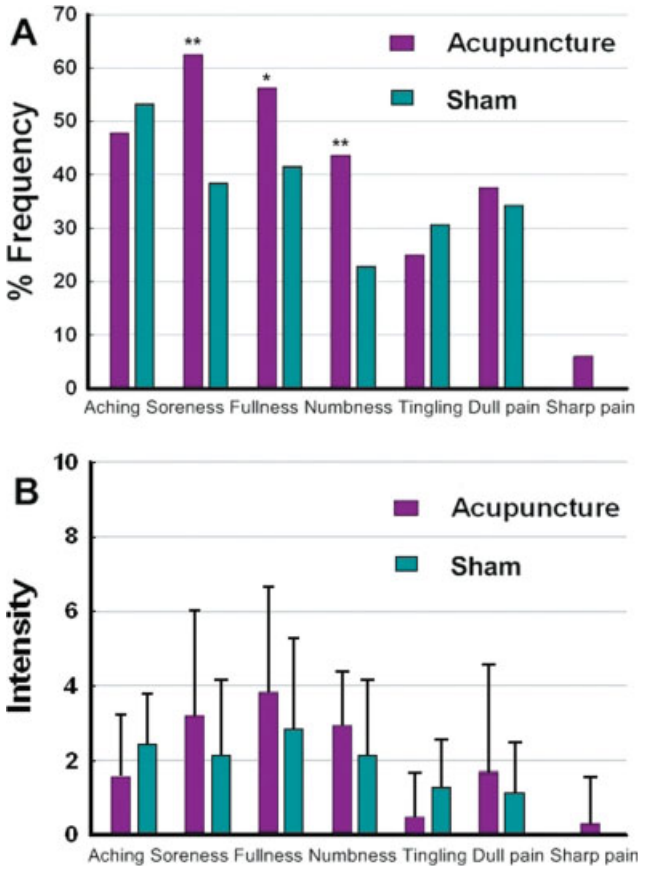

Figure 2.

Averaged psychophysical response ($N = 16$). (**A**) The percentage of subjects who reported having experienced the given sensation (at least one subject experienced the seven sensations listed). The occurrence frequency of numbness, fullness, and soreness was found greater for the ACUP under Fisher's exact test ($*P < 0.01$, $**P < 0.005$). (**B**) The intensity of reported sensations measured by an average score (with standard error bars) on a scale from 0 denoting no sensation to 10 denoting an unbearable sensation. The average stimulus intensities (mean ± SE) were approximately similar during acupuncture at the ST36 (2.4 ± 1.7) and NMP (2.2 ± 1.9). [Color figure can be viewed in the online issue, which is available at www.interscience.wiley.com.]

TABLE I. Significant changes in signal intensity derived from different epochs versus baseline condition during visual stimulation (df = 9, $P < 0.005$ uncorrected)

		V1 vs. BL					R1′ vs. BL					V2 vs. BL					R2′ vs. BL				
		Talairach			*t*	*V*	Talairach			*t*	*V*	Talairach			*t*	*V*	Talairach			*t*	*V*
		x	*y*	*z*	Value	(mm^3)	*x*	*y*	*z*	Value	(mm^3)	*x*	*y*	*z*	Value	(mm^3)	*x*	*y*	*z*	Value	(mm^3)
Occipital lobe																					
Cuneus	L	−9	−93	5	6.73	1,080						−3	−72	15	4.15	324					
BA 17	R	15	−95	19	4.64	405						6	−90	5	4.34	135					
IOG/LG	L	−6	−93	2	6.46	1,809						−42	−73	−4	5.71	324					
BA 18	R	3	−84	2	5.50	486						3	−87	2	4.78	351					
MOG/FG	L	−18	−98	16	5.34	1,431						−42	−74	−14	6.01	513					
BA 19	R	30	−87	2	5.06	621															
Temporal lobe																					
STC/MTC	L	−45	−43	21	4.64	108															
BA 22/37	R	48	8	−16	3.85	108	42	12	−18	3.91	135	62	−12	0	4.57	729	63	−21	0	3.33	108
Parietal lobe																					
IPC/precuneus	L	−27	−53	50	3.92	108						−21	−50	44	5.64	945					
BA 40/7	R											42	−36	43	4.88	972	12	−72	26	4.35	135
PCG	L	−39	−27	46	3.85	135															
BA 3	R																				

BA, brodmann area; IOG, inferior occipital gyrus; LG, lingual gyrus; MOG, middle occipital gyrus; FG, fusiform gyrus; STC, superior temporal cortex; MTC, middle temporal cortex; IPC, inferior parietal cortex; PCG, postcentral gyrus.
Positive activations were seen mostly in the striate cortex and enhanced activity in the extrastriate cortices during the visual stimulation epochs (V1/V2 vs. BL). By contrast, the general content, remained in the rest epochs (R1′/R2′ vs. BL), rarely contained significant task-related effects, and returned to near-baseline levels. Note that the sustaining responses were primarily located in the cerebellum. Since the subjects were asked to keep immobility during the whole scanning. It was natural that activations of cerebellum, as a key center of monitoring and regulating motor process, may sustain during the whole scanning.

occurring relatively high during repetition of simple tasks.

To verify whether the rest epochs (R1′ and R2′) embodied the visual stimulation associated effects, we further compared the signal changes during the R1′ or R2′ with the BL, respectively. Results indicated that the general content of the rest epochs (R1′ and R2′) did not contain significant task-related effects, but maintained similar to each other, regardless of the prior visual stimulation. In addition, there was an excellent correlation between the timing of the onset and offset of visual stimulus, and the variation of signal intensities in some task-related brain regions (shown in Fig. 3C). Note that the BOLD signal returned to near-baseline values shortly after the visual stimulus.

fMRI Results of Acupuncture Stimulation Versus Resting Epochs

Group results during acupuncture on ST36 displayed distinct patterns of hemodynamic responses between two sequential stimulation blocks (Figs. 3A and 4). The first acupuncture stimulation (A1) compared to the baseline (BL) produced extensive signal increases in the limbic/paralimbic, neocortical regions, brainstem and cerebellum, such as the ipsilateral amygdala (Amy), contralateral parahippocampus (PH)/hippocampus (Hipp), bilateral dorsal anterior cingulate (dACC), bilateral hypothalamus (Hyp), bilateral substania nigra (SN), bilateral secondary somatosensory cortex (SII), frontal/temporal cortex, and anterior/posterior part of cerebellum. In contrast, the BOLD responses of these regions in the second stimulation (contrast "A2 vs. BL") were negative predominantly, except for the anterior insula (AI), somatosensory areas and brainstem that showed focal positive activations (Fig. 4 and Table II). Interestingly, such remarkably similar spatial distributions of increased and decreased activities (presented in A2) were also observed in R1 and R2 (resting epochs after stimulations) compared to BL. Direct comparisons of the BOLD responses during these epochs identified that response activities of many regions derived from rest periods did overlap with the stimulation-induced activations or deactivations in our current findings.

fMRI Results of the Sham Stimulation Versus Resting Epochs

The group data of the hemodynamic response to the stimulation at an NMP under different epochs also exhibited the long-lasting effects in some brain regions, mainly

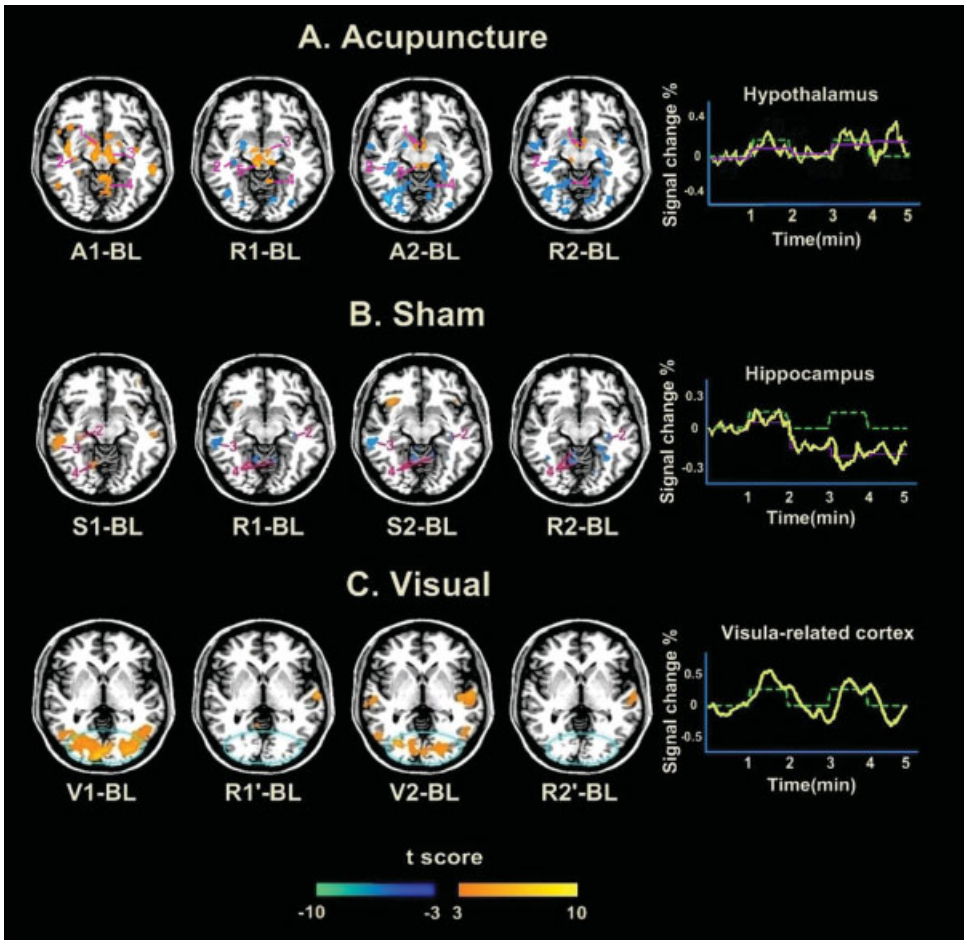

Figure 3.

Group results of brain activation patterns for acupuncture, sham, and visual stimulations in sequential epochs. Statistical significance was thresholded at $P < 0.005$ (uncorrected) and a minimum cluster size of three voxels. Representative color-coded statistical maps under different epochs exhibited the distribution of foci with significant increases (shown in the spectrum from orange to yellow) and decreases (shown in blue), relative to the respective baseline condition BL. (**A**) Group results from 15 subjects undergoing acupuncture at ST36 were shown in an axial section ($Z = -10$ mm). Regions: 1, hypothalamus; 2, hippocampus; 3, substania nigra; 4, cerebellum; 5, periaqueductal gray. The relatively intermittent increased activity was exhibited in the hypothalamus; this pattern seemed anomalous, as the greatest signal change was not consistent with acupuncture stimulation condition. (**B**) Group results from 15 subjects undergoing the stimulation on NMP were also shown in axial section ($Z = -10$ mm). Regions: 2, hippocampus; 3, middle temporal gyrus; 4, cerebellum. Note that the averaged time course of normalized signal intensity in the hippocampus presented a saliently decreased tendency, with a poor correlation with the experiment paradigm. (**C**) Group results from 10 subjects undergoing the visual stimulation were presented in an axial slice ($Z = 1$ mm). Positive activations were seen mostly in the striate cortex and enhanced activities in the extrastriate cortices during visual stimuli (V1/V2 vs. BL). In addition, the general content of the rest epochs (R1′/R2′ vs. BL) did not contain significant task-related effects, and returned to near-baseline level after the stimulus phase. Note that the averaged time course from activated regions within the blue circle yielded a high correlation with the experiment paradigm. [Color figure can be viewed in the online issue, which is available at www.interscience.wiley.com.]

in the contralateral PH/Hipp, bilateral AI, sensorimotor cortex (secondary somatosensory cortex, SII), and cerebellum, with relatively small extent of spatial distributions and less intensive signal changes compared to ST36 (Figs. 3B and 5). As illustrated in Table III, these structures presented marked positive signal changes in the phase S1, but negative predominantly in sequential epochs (R1, S2, and R2). Predictably, the SII demonstrated relatively stable signal increase for all the epochs. However, no significant changes were detected in the major structures of the limbic-related and brainstem regions (Amy; Hyp; perigenual ACC, pACC; periaqueductal gray, PAG; SN; red nucleus,

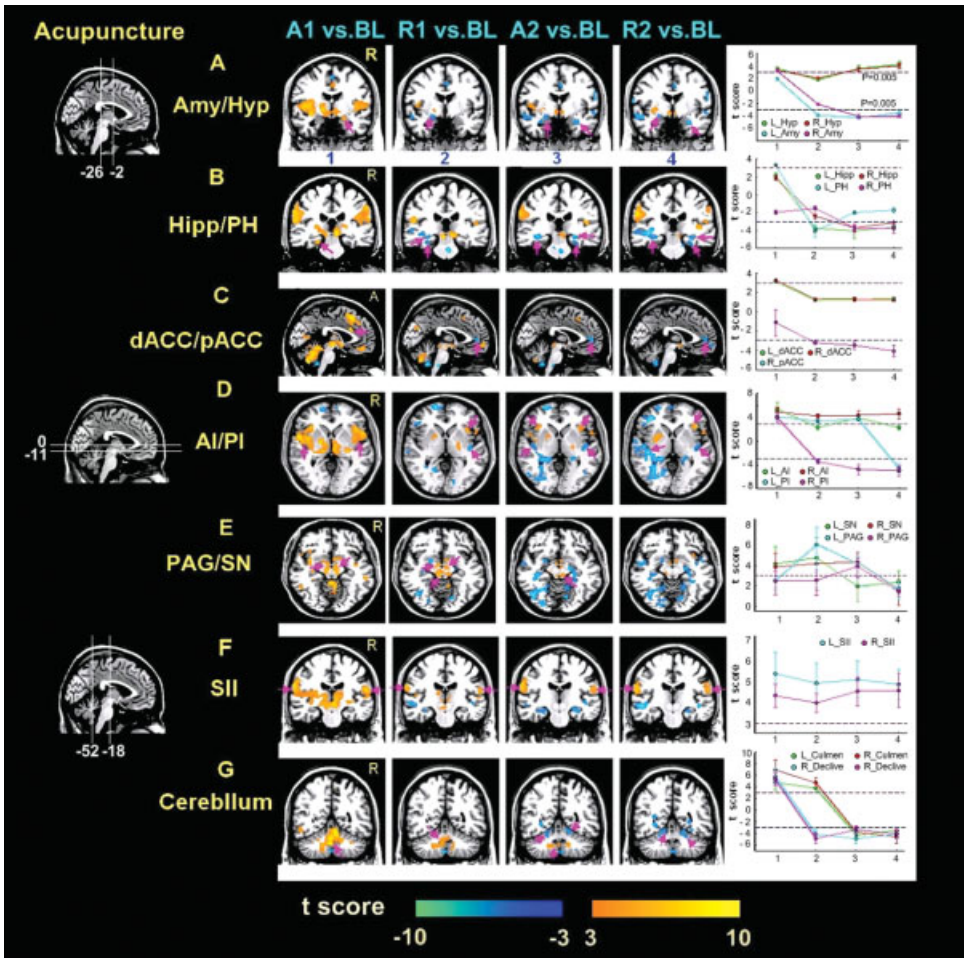

Figure 4.

Activity patterns of representative areas under different epochs during acupuncture stimulation on ST36. Result maps were derived from the same data sets presented in Figure 3A using the same criteria ($P < 0.005$ uncorrected with at least three voxels). Regions of interest were denoted by amaranth arrowheads. Corresponding *t* values of representative regions under different periods were also indicated (Error bars SEM). (**A**,**B**) The amygdala (Amy), hippocampus (Hipp), and parahippocampus (PH) presented weakly positive responses in the first stimulation A1, but decreased to the below-baseline level thereafter. (**C**) Early positive signal response was particularly located in the dorsal part of the ACC, and negative in the pregenual part in sequential conditions. (**D**,**F**) The insula (both anterior and posterior part, AI and PI) and secondary somatosensory cortex (SII) indicated relatively persistent increased responses during the whole trial. Note that signal changes in the SII during needling manipulations (A1 and A2) were relatively higher than that of rest epochs (R1 and R2). (A,**E**) Episodic responses were primarily distributed in the hypothalamus (Hyp), and brainstem structures (periaqueductal gray, PAG; substania nigra, SN). As shown in the PAG, the greatest positive activity emerged in the R1, plateaued in the A2, but showed no significant activity in both A1 and R2 conditions. (**G**) The BOLD responses in the cerebellum (anterior part, culmen; posterior part, declive) were positive predominantly, and negative afterwards. [Color figure can be viewed in the online issue, which is available at www.interscience.wiley.com.]

RN), contrasting with hemodynamic responses to the acupuncture stimulation at ST36.

Elevated Activity During "Rest" and Its Influence on Signal Detections

Studies on acupuncture at commonly used acupoints have demonstrated significant signal changes in wide brain regions; however, few studies detected the PAG activity using BOLD fMRI [Liu et al., 2004]. Apart from this observation, the pattern of signal changes in the Hyp has also been reported with contradictory results [Hui et al., 2005; Wu et al., 1999]. Although such discrepant findings may be partly due to the various factors involved in the experiments, such as different acupoints used, different needling methods, and diverse intensities of acupuncture

TABLE II. Foci with significant changes in signal changes derived from different epochs versus baseline condition during acupuncture at right ST 36 (d.f. = 14, P < 0.005 uncorrected)

		A1 vs. baseline					R1 vs. baseline					A2 vs. baseline					R2 vs. baseline				
		Talairach			*t*	*V*	Talairach			*t*	*V*	Talairach			*t*	*V*	Talairach			*t*	*V*
		x	*y*	*z*	Value	(mm^3)	*x*	*y*	*z*	Value	(mm^3)	*x*	*y*	*z*	Value	(mm^3)	*x*	*y*	*z*	Value	(mm^3)
Limbic system																					
Amygdala	L						−26	0	−15	4.16	108	−28	−5	−18	−4.64	135	−22	0	−15	−3.76	108
	R	18	−6	−12	3.37	135						27	−6	−21	−4.48	108	28	−3	−22	−4.28	108
PH/Hipp	L	−28	−26	−20	3.51	189	−15	−38	2	−4.73	243	−30	−12	−18	−5.54	459	−30	−13	−17	−3.85	162
	R											26	−27	−16	−4.12	729	27	−27	−19	−4.43	567
Dorsal ACC	L	−6	27	23	3.26	189															
BA 32	R	4	32	22	3.42	162															
Perigenual ACC	L																				
BA 24	R						6	45	3	−3.41	216	6	44	2	−3.59	108	6	42	1	−4.60	135
MCC/PCC	L	−3	−19	36	4.47	594															
BA 32/23	R	4	−45	26	5.83	486															
Hypothalamus	L	−3	−3	−9	3.14	135						−3	−6	−8	3.56	135	−3	−3	−7	5.81	108
	R	4	−6	−7	3.28	108						3	−4	−9	3.43	108	3	−4	−8	4.33	108
Anterior insula	L	−39	20	2	6.09	486						−36	21	3	4.12	162					
BA 13	R	36	20	3	4.45	621	34	21	2	4.48	216	39	19	0	4.63	297	44	13	4	4.81	216
Posterior insula	L	−42	−2	−5	5.29	1998						−43	−2	0	3.89	108					
	L											−42	−21	2	−9.37	135	−43	−15	−2	−5.24	189
BA 13	R	42	−14	−5	5.54	1566	42	−18	3	−4.02	162	45	−14	3	−5.12	135	42	−17	3	−5.62	351
Subcortical																					
Thalamus	L	−9	−29	7	4.55	1215															
	R	6	−14	9	5.45	1539															
Brainstem																					
SN/RN	L	−3	−18	−4	6.17	486	−15	−21	−6	3.56	567										
	R	3	−18	−4	6.51	324	12	−18	−9	3.82	324	12	−21	−9	3.24	162					
PAG	L						−4	−29	−9	6.31	486	−4	−29	−12	5.96	135					
	R											3	−28	−8	3.74	189					
RVM	L						−2	−36	−40	−4.31	405	−2	−33	−41	3.09	108					
	R						2	−33	−41	−7.34	162	2	−36	−40	−4.73	297					
Sensorimotor																					
SI	L	−15	−33	71	4.53	297															
BA 3	R																				
SII	L	−50	−30	32	6.05	2781	−62	−20	14	5.50	297	−62	−25	29	5.78	1944	−57	−29	23	5.78	1080
BA 40	R	53	−28	32	4.85	1890	56	−28	18	4.38	108	52	−27	19	3.51	108	56	−26	21	5.22	702
SMA	L																−3	14	55	4.12	135
BA 6	R	4	−18	56	7.23	405						3	−20	49	4.02	108					
Frontal cortex																					
OFC/MPFC	L	−4	43	−8	5.32	594											−5	48	−12	−5.57	297
BA 10/11	R	5	41	−14	6.03	540	4	48	−11	4.30	297						4	48	−19	−3.85	135
DLPFC/VLPFC	L	−29	29	−9	6.80	1215						−56	12	13	−4.91	540	−36	29	−4	−4.73	459
BA 9/44/45	R	56	13	19	5.40	1512						56	13	21	−3.59	189	56	13	21	3.24	270
Temporal cortex	L	−54	−57	−12	4.50	594						−56	−55	−14	−5.10	675	−55	−22	−14	−5.18	891
BA 21/20	R											54	−54	−10	−4.96	270	44	−55	−15	−4.67	270
Parietal Cortex																					
IPC/precuneus	L	−56	−24	30	5.87	1620	−57	−30	28	−4.39	270	−24	−72	36	−4.46	351	−63	−27	30	−5.21	918
BA 40/19	R	59	−26	33	4.83	1188	45	−39	45	−4.03	297	24	−70	39	−4.93	243	24	−75	39	−4.73	297
Occipital cortex	L	−3	−67	6	5.28	405	−18	−84	7	−5.74	648	−27	−70	−9	−7.33	1647	−27	−61	1	−5.81	2349
BA 18/19	R	6	−71	31	3.87	540	18	−78	6	−4.47	567	18	−81	12	−6.24	972	18	−84	15	−6.27	1755
Cerebellum																					
Culmen	L	−3	−57	−30	6.79	2511	−3	−54	−27	4.27	625	−3	−48	−21	−4.10	351	−4	−54	−18	−3.74	567
	R	6	−57	−21	9.15	2457	6	−54	−27	5.23	625	4	−57	−30	−3.12	270	9	−63	−6	−5.10	972
Declive	L	−15	−60	−18	6.48	2133	−18	−63	−21	−4.17	513	−33	−63	−18	−4.87	135	−36	−66	−21	−4.21	108
	R	18	−66	−12	6.16	1782	15	−78	−18	−4.98	625	21	−57	−15	−3.09	162	15	−75	−18	−3.92	135

BA, Brodmann area; PH, parahippocampus; Hipp, hippocampus; ACC, anterior cingulate cortex; MCC, middle cingulate cortex; PCC, posterior cingulate cortex; SN, substania nigra; RN, red nucleus; PAG, periaqueductal gray; RVM, rostral ventromedial medulla; SI, primary somatosensory cortex; SII, secondary somatosensory cortex; SMA, supplementary motor area; OFC, orbitofrontal cortex; MPFC, medial prefrontal cortex; DLPFC, dorsolateral prefrontal cortex; VLPFC, ventrolateral prefrontal cortex; MTC, medial temporal cortex; FG, fusiform Gyrus; IPC, inferior parietal cortex.

The coordination of voxel with the maximal signal change within each region was listed. Red color denoted the positive activation, and blue for negative. The initial acupuncture administration elicited a predominant pattern of signal increases in the cerebrum, brainstem and cerebellum. By contrast, in later epochs (R1, A2 and R2), most of limbic regions and cerebellum presented below-baseline activities. Notably, the hypothalamus, sensorimotor cortex and brainstem showed predominantly above-baseline responses through the whole scanning.

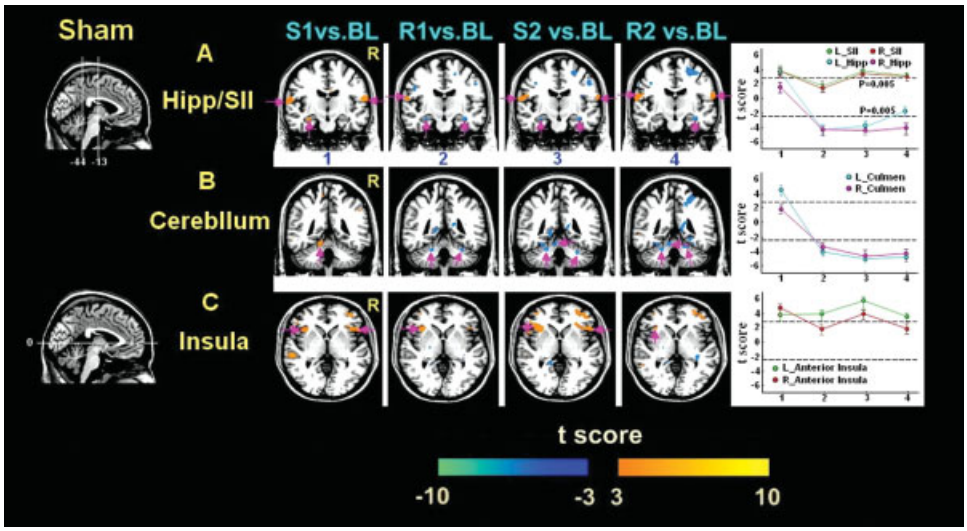

Figure 5.
Time-varying signal changes in the Hipp, SII, and cerebellum under different epochs of acupuncture at the NMP. [Color figure can be viewed in the online issue, which is available at www.interscience.wiley.com.]

stimulation, we further hypothesized that such varied patterns of detected hemodynamic responses (either null activity or reversal sign) may also be attributed to the presence of significant activities during the interleaved "rest" periods in the block-design. Note that previous studies always adopted these rest epochs as the baseline for the comparison with the signal intensity during the stimulation. In this study, we attempted to detect the varied magnitude of the response within the PAG and Hyp, when adopting alternative conditions as the baseline. Here, a region within the PAG in the A2 phase can be identified with significantly increased activity, when employing BL as the baseline (Fig. 6A). However, when R1 was used as the baseline, the PAG was not associated with detected activity changes. In this case, the "rest" condition was apparently an active condition associated with significant stimulus-related activity. Some early failures to observe activity in this area, therefore, might have resulted from the use of an inaccurate "resting" condition. It should also be mentioned that not only can activity during a baseline condition serve to reduce or eliminate the BOLD response, but also such baseline activity can reverse its sign. It was so intriguing that activity in the Hyp during the R2 phase was greater than that of the A1 phase (Table II). Therefore, the hemodynamic response of the Hyp was positive when the BL was used as a baseline, but negative when the R2 was used as a baseline (Fig. 6B). In this case, the presence of significant activity during the "rest" served to reverse the sign of the activity during the conditions of interest. Although it was likely that the relaxed fixation periods used for resting state represent a reasonable estimate of "baseline activity" in the visual task (Fig. 3C), this was not the case when acupuncture considered.

DISCUSSION

This is a systematic study on the sustained central effect of acupuncture and its influence on fMRI signal detections when a block-design paradigm being used. Numerous fMRI studies have used the block-design paradigm to explore the conditions of interest in classic visual or sensorimotor tasks; the corresponding visual or sensorimotor cortical areas are assumed to be activated almost simultaneously, and their BOLD signals return to near-baseline values shortly after stimulation. Such "on-off" hemodynamic response patterns were again corroborated by our fMRI results from a block-designed visual task. However, the temporal feature of the acupuncture indicated in this study differed markedly from those of conventional block-designed tasks. Interestingly, we found prominently stimulus-related activities in the extensive cerebro-cerebellar and limbic brain regions (as well as brainstem structures) in the "resting" periods even after acupuncture stimulation terminated.

Intertrial Interval Activities Do Not Reflect Passive Ongoing Processes

For acupuncture at ST36, there were saliently prolonged activities during the intertribal intervals or nonstimulus resting states. However, spatial distributions of such delayed responses were different from that of the internal processing sources, which are most prominent in the midline dorsal/ventral frontal cortex and the posterior cingulate cortex [Raichle and Snyder, 2007; Raichle et al., 2001].

TABLE III. Foci with significant changes in signal changes derived from different epochs versus baseline condition during sham acupuncture at nonacupoint (df = 14, $P < 0.005$ uncorrected)

		S1 vs. baseline					R1 vs. baseline					S2 vs. baseline					R2 vs. Baseline				
		Talairach			*t*	*V*	Talairach			*t*	*V*	Talairach			*t*	*V*	Talairach			*t*	*V*
		x	*y*	*z*	Value	(mm^3)	*x*	*y*	*z*	Value	(mm^3)	*x*	*y*	*z*	Value	(mm^3)	*x*	*y*	*z*	Value	(mm^3)
Limbic/paralimbic																					
PH/Hipp	L	−27	−13	−17	3.83	135	−30	−12	−17	−3.98	162	−24	−36	−13	−3.59	189					
BA 35/36	R						27	−27	−19	−4.06	135	27	−27	−19	−4.39	324	33	−15	−17	−4.15	216
Anterior insula	L	−30	17	−6	3.77	432	−30	17	−6	3.92	162	−30	17	−6	5.86	162	−36	22	0	3.62	162
BA 13	R	33	21	13	4.53	297						36	−8	14	3.89	243					
Posterior insula	L	−50	−31	21	4.47	270											−30	−28	18	−3.40	135
BA 13	R																42	−11	17	−4.05	189
Sensorimotor																					
SI	L																				
BA 2	R	39	−30	66	3.25	189						45	−29	53	−3.73	216	45	−26	51	−3.96	324
SII	L	−53	−28	21	3.86	594	−59	−5	17	3.21	189	−59	−28	21	3.98	729	−62	−8	14	3.44	459
BA 40	R	59	−28	21	3.72	540						45	18	7	3.70	135	48	−21	45	3.65	540
OFC/MPFC	L	−48	21	−7	3.59	297						−3	14	44	−4.12	162					
BA 6/32	R	4	41	−14	4.71	243	4	44	−9	−4.56	189	13	28	32	4.18	216	4	45	−14	−4.45	135
DLPFC/VLPFC	L	−45	10	27	5.13	783						−30	20	−9	5.87	216	−30	20	−9	−4.18	378
BA 9/45	R	39	47	0	4.24	729	56	4	27	−4.37	108						50	−2	19	−4.86	270
IPC/precuneus	L	−50	−28	24	4.10	1026											−21	−75	23	−3.92	189
BA 40/7	R						30	−47	49	−3.94	189	30	−47	52	−3.51	243	30	−47	53	−4.50	135
Temporal cortex	L	−53	−29	−1	6.47	378						−30	−39	−16	−4.09	297	−30	−44	−13	−3.47	162
BA 20/21	R	62	−24	−6	3.13	162						33	−39	−18	−3.62	324	36	−39	−16	−5.28	405
Cerebellum																					
Culmen	L	−27	−39	−16	4.46	243	−24	−39	−18	−3.94	432	−24	−39	−18	−5.66	216	−18	−45	−23	−4.75	189
	R						27	−39	−18	−3.41	189	21	−41	−13	−4.58	135	21	−50	−18	−4.82	216
Declive	L											−12	−59	−15	−3.55	162	−9	−56	−12	−3.80	135
	R	12	−74	−24	3.77	459															

BA, Brodmann area; PH, parahippocampus; Hipp, hippocampus; MCC, middle cingulate cortex; SI, primary somatosensory cortex; SII, secondary somatosensory cortex; MPFC, medial prefrontal cortex; OFC, orbitofrontal cortex; DLPFC, dorsolateral prefrontal cortex; VLPFC, ventrolateral prefrontal cortex; IPC, inferior parietal cortex.
The coordination of voxel with the maximal signal change within each region was listed. Red color denoted the positive activation, and blue for negative.

Intriguingly, more complicated bidirectional responses (below-baseline activities in the Amy, Hipp, PH, pACC and above-baseline activities in the Hyp, AI, and brainstem structures) were found in the "rest" periods following acupuncture. One interpretation of such wide range of activities may be derived from the long-acting effects of acupuncture. More importantly, the temporal response of some areas (the Amy, Hipp, and PH) during the "rest" periods even turned to an inverse direction.

Acupuncture-Related Activity in the Rest Epoch—A Nonoptimal Baseline

Given that fMRI analysis is an inherently contrastive methodology [Ogawa et al., 1990], the presence of activity during the baseline condition can seriously compromise the integrity of the sequential results. This is exemplified in the fact that using this rest condition as a baseline often made it difficult to observe activity during memory tasks [Buckner et al., 1995; Shallice et al., 1994], and difficult to obtain appropriate interpretations about the activity when it is observed [Binder et al., 1999]. Likewise, if rest period actually contained stimulus-related effects due to the slow-acting agent of acupuncture, such rest epoch may be far from a control condition but an apparently active one. Consequentially, neural activities during rest periods may reduce, eliminate, or even reverse the sign of activities during stimulation conditions.

The fact of the matter was that, throughout much of the PAG, the rest R1 was associated with approximately the same level of activity as the acupuncture stimulation A2 (Table II). In this case, rest was apparently an active condition associated with significant stimulus-related activities. Some early failures to observe activity in the PAG may have occurred when the acupuncture stimulation was contrasted with such a rest condition. Even in a recent study that successfully detected the activity of PAG, reliable activation was obtained after 20 min of acupuncture stimulation ($P < 0.05$, uncorrected) [Liu et al., 2004]. And they speculated that undetected activity of the PAG in other studies may be due to the short period of stimulation

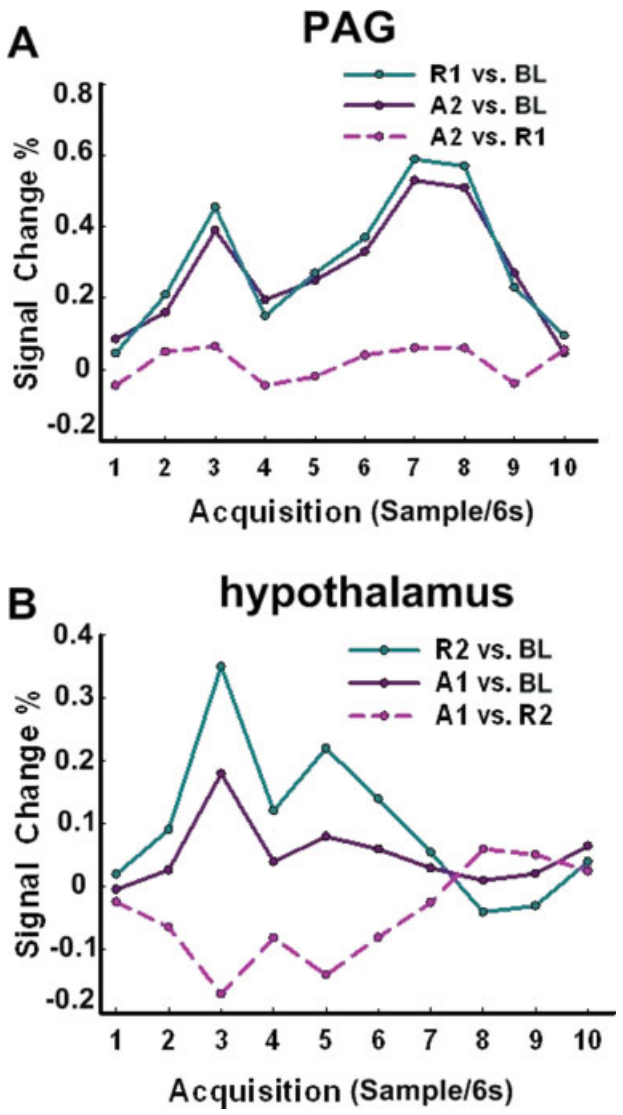

Figure 6.

Hemodynamic response showing activity over time (resampled at 6 s) in the specific brain region following acupuncture at ST36. (**A**) Activity in the contralateral PAG. When the BL epoch was used as the baseline, the PAG was associated with significantly increased activity under the stimulation phase A2. In contrast, when the R1 was used as the baseline, no detectable activity was identified. B. Activity in the contralateral hypothalamus. The A1 was associated with significantly increased activity in the hypothalamus when BL was used as a baseline. However, when the rest R2 was used as a baseline, the stimulus A1 was associated with saliently decreased activity. Therefore, the effect of activity during the rest condition can eliminate, or even reverse the sign of the activity during the conditions of interest. [Color figure can be viewed in the online issue, which is available at www.interscience.wiley.com.]

paradigm. In contrast, the PAG in our study was activated twice and presented more robust increased activations during a shorter 5 min test sequence ($P < 0.005$, uncorrected) (Fig. 4E and Table II). Although such discrepancy might partly be derived from the acupuncture stimulation at different acupoints (LI4 vs. ST36) or other methodological differences, one potential difference may be attributed to the utilization of interleaved rest periods as the contrast baseline; the activity of the PAG would be hidden, owing to elevated activities in the rest period (as shown in Fig. 6A). Moreover, the presence of significant activities during the rest R2 can reverse the sign of the Hyp activity during the conditions of interest A1 (Fig. 6B). Altogether, the ambiguity of such rest condition made it not so ideal to serve as a baseline for comparison with acupuncture stimulations.

Deactivation Tendency in Pain-Related Limbic-Cerebellar Areas as Time Prolonged

Results in this study also supported the view that the kinetics of acupuncture was complex and longer acting as a function of time, rather than a simple variation in the block-based response amplitudes (see Fig. 4). In other words, another important dimension that deserved more attentions in acupuncture studies was the temporal duration of information representation itself.

Our findings unveiled that acupuncture at ST36 induced a notable feature of time-varying and bidirectional responses in the wide limbic-cerebellar areas, BOLD signal increased in the first stimulation epoch and decreased gradually to reach significance below the baseline level (Table II). For the NMP, this pattern of temporal response was only presented in the PH/Hipp and cerebellar, but absent in other major limbic regions (such as the Amy and pACC) (Table III). The Amy mainly supported the encoding of affective aspects of pain [Toelle et al., 1999]. Signal attenuation in the Amy is also observed to be correlated with the elevation of pain threshold in subjects [Zhang et al., 2003].

For acupuncture at ST36, another notable finding was the saliently time-dependent responses in different parts of the ACC: early increased signal response was mainly located in the dorsal part, and inhibited in the pregenual part during the sequential conditions (Fig. 4C). This finding was partly consistent with the functional division of the ACC: notably, the metabolic activation of the ACC by pain [Casey, 1999; Talbot et al., 1991] or by more specific aspects of the pain experience, such as the pain intensity [Hofbauer et al., 2001; Talbot et al., 1991], pain anticipation [Ploghaus et al., 1999], the illusion of pain [Craig et al., 1996], or even empathy to pain experienced by others, has typically involved more dorsal subregion of the ACC [Jackson et al., 2005]. Conversely, the metabolic activity of the pACC has been traditionally implicated in modulation

of the pain experience responses, the affective qualities [Toelle et al., 1999], and more recently, in the placebo effect [Wager et al., 2004]. In addition, the pACC always showed delayed responses when compared with other regions in the temporally resolved fMRI data [Cho et al., 2003], suggesting its functional role in the pain modulation. The dorsal-pregenual dimension within the ACC might be organized in the length of time, according to the temporal duration of actively maintained representations.

Physiologically, deactivation can be interpreted as the suppression of neuronal activity in a given condition relative to the control condition caused by decreased firing, decreased temporal synchronization of firing, or recruitment of neurons [Fransson et al., 1999]. On the whole, the limbic-cerebellar regions own necessary properties to play key roles in both affective and motoric pain processing [Helmchen et al., 2003; Price, 2000], and also in ascending pain-conductive system and endogenous anti-nociceptive signaling [Treede et al., 2000]. This evidence converged with one notion that pain-processing areas were desensitized due to the acupuncture stimulation.

Deactivated Regions Overlapped With the Default Mode Network

Aside from the limbic-cerebellar brain network, the time-prolonged signal attenuations induced by acupuncture stimulation at both ST36 and NMP distributed in a much larger set of brain regions, namely the medial temporal cortices, the orbitofrontal cortex bilaterally, large sections of the occipital cortex, the medial prefrontal cortex, large sections of the frontal cortex (dorsolateral prefrontal cortex, DLPFC; ventrolateral prefrontal cortex, VLPFC), and the parietal cortex (precuneus; inferior parietal cortex, IPC) (Tables II and III); these areas included the majority of structures, commonly deactivated across a wide range of tasks and stimulus modalities [Raichle et al., 2001]. The leading hypothesis regarding the functional meaning of this phenomenon suggests the network of regions underlying a "default mode" of brain activity, which is mainly present at rest and strongly attenuated during various goal-directed tasks. In other words, during a novel and specific task, processing resources are moved from the areas normally engaged in the "default mode" to the areas relevant for the presented task [Gusnard et al., 2001]. Likewise, acupuncture is, at any rate, an intervention procedure, and its procedural administration manifests mainly as highly focused attentions. Such larger extent of deactivated areas may suggest a greater shift of processing resources toward a stronger and more attentionally demanding stimulus.

Signal Sustained Across the Entire Session

As discussed earlier, acupuncture induced large distributions of time-phased or time-varied BOLD responses, whereas relatively persistent activities can be also identified in the SII and insula at both ST36 and NMP (Figs. 4 and 5). BOLD signal increases in the SII and insula were also the most consistently observed findings and were reported, regardless of acupoint location or acupuncture mode [Hui et al., 2000, 2005; Napadow et al., 2005; Pariente et al., 2005; Wu et al., 1999]. From the examination of the physiological data, it was notable that acupuncture needling sensations, combining soreness, dull pain and deep, unusual somatosensations, could persist long after the peripheral stimulation had been conducted. Recent fMRI studies of pain in humans have substantiated the role of the SII in sensory-discriminative aspects, demonstrating that this area is considerably involved in intensity coding of applied and perceived pain [Hofbauer et al., 2001; Willer, 1977]. Therefore, it was not surprising to observe the sustained response in this sensorimotor-related region through the whole scanning session. On the other hand, it also seemed reasonable that activities related to the maintenance of the homoeostasis state might sustain throughout the performance of the task. Underpinning this role of the insula as a core center is its status of multimodal convergences and its coordination between our internal milieu with the extrapersonal space. The insula cortex has wide connections with the somatosensory areas, ACC, amygdaloid body, prefrontal cortex, temporal pole, orbitofrontal cortex, frontal operculum, hypothalamus, and brainstem structures [Chikama et al., 1997]. Its abundant connections and functional interface between the limbic system and the neocortex place it in a unique position to assign significance to the sensory information it receives [Mesulam and Mufson, 1982]; to possibly effect decisions and subsequent behavior [Casey, 1999; Damasio et al., 2000]. Considering that acupuncture may mediate the neurophysiological system with more voluntary components of self-control and self-regulate to restore homoeostasis, the insula, as an alarm center for internally-sensed changes, may engage in monitoring the ongoing modulation of acupuncture effect on the internal states of the organism.

Episodic Responses Only Presented During Acupuncture at ST36 but Not NMP

Besides the examination of the neural substrates involved during both stimulation conditions, this study also identified several important brain areas only modulated during the acupuncture stimulation on ST36. The regions, including the PAG, rostral ventromedial medulla (RVM), and Hyp, presented significantly intermittent activities (Fig. 4A,E and Table II). As shown in the PAG, the greatest magnitude of activity emerged in the R1 (18 voxels, $t = 6.31$), plateaued under A2 (5 voxels, $t = 5.96$), but indicated no significant activities on the later condition. At the first blush, this pattern seems anomalous, as the greatest signal change was not consistent with the stimulation condition.

The PAG plays a key role in descending mechanisms by controlling the transmission of nociceptive signals to the brain [Willis, 1985]. One of these mechanisms by which the PAG modulates the ascending sensory responses involves releasing endogenous opioids to exert its antinociceptive effect through the opioid synapses of the RVM system [Fields and Basbaum, 1999]. The RVM has distinct but anatomically overlapping populations of modulatory neurons: off cells that inhibit and on cells that facilitate nociceptive transmission [Haws et al., 1989]. This could partially explain the RVM showed more complex (bidirectional) activity patterns in our findings (Table II). Cells throughout this network could always fire simultaneously, implicating the PAG-RVM network functions as a unit and exerting discrete control, globally rather than topographically, over dorsal horn pain transmission neurons. In addition, the increased activation of the Hyp further corroborated previous findings [Hsieh et al., 2001; Wu et al., 1999]. Although unable to provide direct evidence from this study, we speculated that acupuncture stimulation at the analgesic point (ST36) may engage major structures of the descending antinociceptive system, particularly the Hyp, PAG, and RVM, proving its important roles for potential efficacy.

Compared with a NMP, acupuncture at ST36 induced significantly complex response patterns with a larger extent of spatial distributions and relatively more robust magnitudes. These notable BOLD signal changes shared a common feature that the identified voxels, containing a population of neurons, coded the temporal dimension [Faingold and Randall, 1995; Petrovic et al., 2004; Quirk and Mueller, 2008]. Some regions only responded to the initial administration of acupuncture, and others may ramp up or taper off across the whole session. Yet other brain areas showed sustained responses, and continuously exerted controlling and coordinated influences throughout the scanning. Even in the same brain region, there were distinct temporal responses reflecting a significant modulation of response directions during different stages of the acupuncture. It was also deserved to mention that not only was such time-varied brain response emerged following the acupuncture but also exhibited during the sham intervention. Because of the same needling manipulation performed on the NMP, it was not surprising that these delayed signal responses was primarily located in the insula, PH/Hipp, SII, and cerebellar, which are generally involved in the nociceptive processing and pain perception [Tracey and Mantyh, 2007]. Meanwhile, significant discrepancies in temporal response patterns of some neural substrates (such as the Amy, pACC, Hyp, and brainstem structures) also existed between two stimulations. Though it was still inadequate to provide direct evidence on the ST36-specific effects (such as analgesic) over NMP, these findings would enlighten the researchers to investigate the neuromodulatory effect of acupuncture, not only from spatial extents but also in temporal dimensions. If acupuncture was a slow-acting agent, the temporal information involved may help further enclose its specific mechanism on brain modulation. Although speculative, this hypothesis was supported by clinical practice that acupuncture can provide prolonged analgesia even after the needling being terminated.

Methodological Implications

The time-varying (or state-related) responses may or may not be specific to acupuncture. This specificity studies also attract much attention from other fields, including fMRI studies of drug effects [Wise et al., 2004], food intake [Liu et al., 2000], memory [Otten et al., 2002], motivation and emotion [Gray et al., 2002]. In these cases, an accurate interpretation of these actions depends on how effectively we can characterize the nature of temporal variations underlying neural activities that give rise to hemodynamic responses, rather than simply detect the occurrence of such changes. Critically, the depiction of dynamic ongoing acupuncture effects would be obtained in the absence of any assumption concerning the shape of the hemodynamic response, whereas the GLM's effectiveness in modeling such state-related activity is limited. It would clearly be more informative to perform inferences directly on the duration of such activation. In this line, a more flexible model, which captures consistencies in activation magnitude but allows for temporal variations, may be a more optimal choice instead. Recently, our group has applied data-driven methods, such as ICA, to model such slowly varying processes of acupuncture, of which the onset time and durations of underlying psychological activity were uncertain [Zhang et al., 2009].

CONCLUSIONS

Our results have provided solid evidence supporting the idea that acupuncture is a slow-acting agent and has a specific pattern of the dynamics for the entire coupled nervous system. Identifying such changes that occur at a particular time period—early or late during acupuncture processes—may shed lights on how such peripheral inputs are conducted and mediated through a neurophysiological system with more voluntary components of self-regulating and self-organizing integrities of the homoeostasis. More importantly, such a concept may open up new ways by which the actual effect of acupuncture can be appropriately studied. This emerging picture indicates that both designing paradigms and statistical models involved in acupuncture studies should be applied with great care.

ACKNOWLEDGMENTS

We thank Dr. Qiyong Gong and the research staff at the West China Hospital for their assistances in carrying out the experiment and data collections.

REFERENCES

Arfanakis K, Cordes D, Haughton VM, Moritz CH, Quigley MA, Meyerand ME (2000): Combining independent component analysis and correlation analysis to probe interregional connectivity in fMRI task activation datasets. Magn Reson Imaging 18:921–930.

Arieli A, Sterkin A, Grinvald A, Aertsen A (1996): Dynamics of ongoing activity: Explanation of the large variability in evoked cortical responses. Science 273:1868–1871.

Bai L, Tian J, Qin W, Pan X, Yang L, Chen P, Chen H, Dai J, Ai L, Zhao B (2007): Exploratory analysis of functional connectivity network in acupuncture study by a graph theory mode. Conf Proc IEEE Eng Med Biol Soc 2007:2023–2026.

Beijing S (1980): Nanjing Colleges of Traditional Chinese Medicine. Essentials of Chinese Acupuncture. Beijing: Foreign Language Press.

Binder JR, Frost JA, Hammeke TA, Bellgowan PS, Rao SM, Cox RW (1999): Conceptual processing during the conscious resting state. A functional MRI study. J Cogn Neurosci 11:80–95.

Buckner RL, Petersen SE, Ojemann JG, Miezin FM, Squire LR, Raichle ME (1995): Functional anatomical studies of explicit and implicit memory retrieval tasks. J Neurosci 15:12–29.

Casey KL (1999): Forebrain mechanisms of nociception and pain: Analysis through imaging. Proc Natl Acad Sci USA 96:7668–7674.

Chikama M, McFarland NR, Amaral DG, Haber SN (1997): Insular cortical projections to functional regions of the striatum correlate with cortical cytoarchitectonic organization in the primate. J Neurosci 17:9686–9705.

Cho ZH, Son YD, Kang CK, Han JY, Wong EK, Bai SJ (2003): Pain dynamics observed by functional magnetic resonance imaging: Differential regression analysis technique. J Magn Reson Imaging 18:273–283.

Craig AD, Reiman EM, Evans A, Bushnell MC (1996): Functional imaging of an illusion of pain. Nature 384:258–260.

Damasio AR, Grabowski TJ, Bechara A, Damasio H, Ponto LLB, Parvizi J, Hichwa RD (2000): Subcortical and cortical brain activity during the feeling of self-generated emotions. Nat Neurosci 3:1049–1056.

Faingold CL, Randall ME (1995): Pontine reticular formation neurons exhibit a premature and precipitous increase in acoustic responses prior to audiogenic seizures in genetically epilepsy-prone rats. Brain Res 704:218–226.

Fang JL, Krings T, Weidemann J, Meister IG, Thron A (2004): Functional MRI in healthy subjects during acupuncture: Different effects of needle rotation in real and false acupoints. Neuroradiology 46:359–362.

Fields HL, Basbaum AI (1999): Central nervous system mechanisms of pain modulation. In: Wall PD, Melzack R, editor. Textbook of Pain. Edinburgh: Churchill Livingstone. pp 309–329.

Fox MD, Snyder AZ, Zacks JM, Raichle ME (2005): Coherent spontaneous activity accounts for trial-to-trial variability in human evoked brain responses. Nat Neurosci 9:23–25.

Fransson P (2006): How default is the default mode of brain function? Further evidence from intrinsic BOLD signal fluctuations. Neuropsychologia 44:2836–2845.

Fransson P, Krüger G, Merboldt KD, Frahm J (1999): MRI of functional deactivation: Temporal and spatial characteristics of oxygenation-sensitive responses in human visual cortex. Neuroimage 9:611–618.

Gray JR, Braver TS, Raichle ME (2002): Integration of emotion and cognition in the lateral prefrontal cortex. Proc Natl Acad Sci USA 99:4115.

Gusnard DA, Raichle ME, Raichle ME (2001): Searching for a baseline: Functional imaging and the resting human brain. Nat Rev Neurosci 2:685–694.

Haws CM, Williamson AM, Fields HL (1989): Putative nociceptive modulatory neurons in the dorsolateral pontomesencephalic reticular formation. Brain Res 483:272–282.

Helmchen C, Mohr C, Erdmann C, Petersen D, Nitschke MF (2003): Differential cerebellar activation related to perceived pain intensity during noxious thermal stimulation in humans: A functional magnetic resonance imaging study. Neurosci Lett 335:202–206.

Hofbauer RK, Rainville P, Duncan GH, Bushnell MC (2001): Cortical representation of the sensory dimension of pain. J Neurophysiol 86:402–411.

Hsieh JC, Tu CH, Chen FP, Chen MC, Yeh TC, Cheng HC, Wu YT, Liu RS, Ho LT (2001): Activation of the hypothalamus characterizes the acupuncture stimulation at the analgesic point in human: A positron emission tomography study. Neurosci Lett 307:105–108.

Hui KK, Liu J, Makris N, Gollub RL, Chen AJ, Moore CI, Kennedy DN, Rosen BR, Kwong KK (2000): Acupuncture modulates the limbic system and subcortical gray structures of the human brain: Evidence from fMRI studies in normal subjects. Human Brain Mapp 9:13–25.

Hui KK, Liu J, Marina O, Napadow V, Haselgrove C, Kwong KK, Kennedy DN, Makris N (2005): The integrated response of the human cerebro-cerebellar and limbic systems to acupuncture stimulation at ST36 as evidenced by fMRI. Neuroimage 27:479–496.

Jackson PL, Meltzoff AN, Decety J (2005): How do we perceive the pain of others? A window into the neural processes involved in empathy. Neuroimage 24:771–779.

Kida I, Hyder F, Kennan RP, Behar KL (1999): Toward absolute quantitation of bold functional MRI. Adv Exp Med Biol 471:681–689.

Liu Y, Gao JH, Liu HL, Fox PT (2000): The temporal response of the brain after eating revealed by functional MRI. Nature 405:1058–1062.

Liu WC, Feldman SC, Cook DB, Hung DL, Xu T, Kalnin AJ, Komisaruk BR (2004): fMRI study of acupuncture-induced periaqueductal gray activity in humans. NeuroReport 15:1937.

Mesulam MM, Mufson EJ (1982): Insula of the old world monkey. 111. Efferent cortical output and comments on function. J Comp Neurol 21:38–52.

Napadow V, Makris N, Liu J, Kettner NW, Kwong KK, Hui KK (2005): Effects of electroacupuncture versus manual acupuncture on the human brain as measured by fMRI. Human Brain Mapp 24:193–205.

Ogawa S, Lee TM, Kay AR, Tank DW (1990): Brain magnetic resonance imaging with contrast dependent on blood oxygenation. Proc Natl Acad Sci USA 87:9868–9872.

Otten LJ, Henson RN, Rugg MD (2002): State-related and item-related neural correlates of successful memory encoding. Nat Neurosci 5:1339–1344.

Pariente J, White P, Frackowiak RSJ, Lewith G (2005): Expectancy and belief modulate the neuronal substrates of pain treated by acupuncture. Neuroimage 25:1161–1167.

Petrovic P, Petersson KM, Hansson P, Ingvar M (2004): Brainstem involvement in the initial response to pain. Neuroimage 22:995–1005.

Ploghaus A, Tracey I, Gati JS, Clare S, Menon RS, Matthews PM, Rawlins JN (1999): Dissociating pain from its anticipation in the human brain. Science 284:1979–1981.

Price DD (2000): Psychological and neural mechanisms of the affective dimension of pain. Science 288:1769–1772.

Price DD, Rafii A, Watkins LR, Buckingham B (1984): A psychophysical analysis of acupuncture analgesia. Pain 19:27–42.

Qin W, Tian J, Pan X, Yang L, Zhen Z (2006): The correlated network of acupuncture effect: A functional connectivity study. Conf Proc IEEE Eng Med Biol Soc 1:480–483.

Qin W, Tian J, Bai L, Pan X, Yang L, Chen P, Dai J, Ai L, Zhao B, Gong Q (2008): FMRI connectivity analysis of acupuncture effects on an amygdala-associated brain network. Mol Pain 4:55.

Quirk GJ, Mueller D (2008): Neural mechanisms of extinction learning and retrieval. Neuropsychopharmacology 33:56–72.

Raichle ME, Snyder AZ (2007): A default mode of brain function: A brief history of an evolving idea. Neuroimage 37:1083–1090.

Raichle ME, MacLeod AM, Snyder AZ, Powers WJ, Gusnard DA, Shulman GL (2001): A default mode of brain function. Proc Natl Acad Sci USA 98:676–682.

Shallice T, Fletcher P, Frith CD, Grasby P, Frackowiak RSJ, Dolan RJ (1994): Brain regions associated with acquisition and retrieval of verbal episodic memory. Nature 368:633–635.

Talairach J, Tournoux P (1988):Co-planar Stereotaxic Atlas of the Human Brain. New York: Thieme Medical Publishers.

Talbot JD, Marrett S, Evans AC, Meyer E, Bushnell MC, Duncan GH (1991): Multiple representations of pain in human cerebral cortex. Science 251:1355–1358.

Toelle TR, Kaufmann T, Siessmeier T, Laurenbacher S, Berthele A, Munz F, Zieglgaensberger W, Willoch F, Schwaiger M, Conrad B (1999): Region-specific encoding of sensory and affective components of pain in the human brain: A positron emission tomography correlation analysis. Ann Neurol 45:40–47.

Tracey I, Mantyh PW (2007): The cerebral signature for pain perception and its modulation. Neuron 55:377–391.

Treede RD, Apkarian AV, Bromm B, Greenspan JD, Lenz FA (2000): Cortical representation of pain: Functional characterization of nociceptive areas near the lateral sulcus. Pain 87:113–119.

Wager TD, Rilling JK, Smith EE, Sokolik A, Casey KL, Davidson RJ, Kosslyn SM, Rose RM, Cohen JD (2004): Placebo-Induced changes in fMRI in the anticipation and experience of pain. Science 303:1162–1167.

Willer JC (1977): Comparative study of perceived pain and nociceptive flexion reflex in man. Pain 3:69–80.

Willis WD (1985): Central nervous system mechanisms for pain modulation. Appl Neurophysiol 48:153–165.

Wise RG, Williams P, Tracey I (2004): Using fMRI to quantify the time dependence of remifentanil analgesia in the human brain. Neuropsychopharmacology 29:626–635.

Worsley KJ, Friston KJ (1995): Analysis of fMRI time-series revisited-again. Neuroimage 2:173–181.

Wu MT, Hsieh JC, Xiong J, Yang CF, Pan HB, Chen YC, Tsai G, Rosen BR, Kwong KK (1999): Central nervous pathway for acupuncture stimulation: localization of processing with functional MR imaging of the brain—Preliminary experience. Radiology 212:133–141.

Wu MT, Sheen JM, Chuang KH, Yang P, Chin SL, Tsai CY, Chen CJ, Liao JR, Lai PH, Chu KA (2002): Neuronal specificity of acupuncture response: A fMRI study with electroacupuncture. Neuroimage 16:1028–1037.

Yoo SS, Teh EK, Blinder RA, Jolesz FA (2004): Modulation of cerebellar activities by acupuncture stimulation: Evidence from fMRI study. Neuroimage 22:932–940.

Zhang WT, Jin Z, Cui GH, Zhang KL, Zhang L, Zeng YW, Luo F, Chen ACN, Han JS (2003): Relations between brain network activation and analgesic effect induced by low vs. high frequency electrical acupoint stimulation in different subjects: A functional magnetic resonance imaging study. Brain Res 982:168–178.

Zhang Y, Qin W, Liu P, Tian J, Liang JM, Deneen KM, Liu YJ (2009): An fMRI study of acupuncture using independent component analysis. Neurosci Lett 449:6–9.